ON THE INTRINSIC INITIATION AND ARREST CLEAVAGE FRACTURE TOUGHNESS OF FERRITE—M. L. Hribernik, G. R. Odette, and M. Y. He (University of California, Santa Barbara)

OBJECTIVE

The primary objective is to assess the hypothesis that a universal master toughness temperature curve shape, $K_{Jc}(T - T_o)$, observed in structural steels derives from an underlying universal temperature dependence of the intrinsic ferrite lattice micro-arrest toughness, $K_\mu(T)$. These results also represent the first database on the fundamental toughness properties of Fe and will provide critical insight on the atomic processes governing the brittle-to-ductile transition (BDT).

SUMMARY

The results of the crack arrest fracture toughness (K_a) measurements on cleavage oriented Fe single crystals from -196 to 0°C are reported. Arrest measurements were performed on four low toughness cleavage orientations; (100)[010], (100)[011], (110)[001] and (110)[110]. Reliable and consistent measurements were obtained for the (100) cleavage planes, however inconsistent measurements were observed for the (110) planes as cleavage cracks always reverted back to the (100) planar orientation. The corresponding static (K_{Ic}) and dynamic (K_{Id}) cleavage initiation toughness for the (100) planes from -196 to 50°C were also measured over a range of applied stress intensity rates ($\dot{K}$) from ≈ 0.1 to 10^4 MPa√m/s. The $K_{Ia}(T)$, $K_{Ic}(T)$ and $K_{Id}(T)$ gradually increase with temperature from a minimum average K_{Ia} value of approximately 4 MPa√m up to a rapid BDT at ≈ 0°C. The BDT temperature increases with higher $\dot{K}$, and is highest for K_{Ia}. The $\dot{K}$ dependence of $K_{Ic/d}(T)$ is consistent with the strain rate dependence of thermally activated flow stress of Fe. The $K_{Ic}(T)$ for single crystal Fe and W are also reasonably similar when plotted on a homologous temperature scale. The $K_{Ia}(T)$ for Fe at ≈ -40°C is similar to that for Fe-3wt%Si at ≈ 110°C. This 150°C shift can be reasonably rationalized by the solid solution lattice strengthening of Si. The $K_{Ia}(T)$ for Fe must be shifted up by ≈ 220°C to approximate the temperature dependence of the $K_\mu(T)$ that is consistent with a universal $K_{Jc}(T)$ master curve shape. This magnitude of shift may be caused by a combination of thermally activated (rate-dependent) solid solution lattice strengthening, complemented by long-range internal stress fields.

PROGRESS ANS STATUS

Introduction

The brittle-to-ductile transition (BDT) in bcc metals and alloys is of both technological and scientific importance. Almost no reliable experimental data are available on the BDT in unalloyed Fe. Also, in spite of a large modeling literature, a fundamental understanding of the BDT remains one of the most elusive material science challenges. A corollary fundamental challenge is to rationalize the empirical observation that the shape of the macroscopic fracture toughness-temperature curve, $K_{Jc}(T - T_o)$, of structural steels is approximately the same when scaled by reference temperature T_o. The universal master curve (MC) shape appears to apply to a very wide range of alloy microstructures and strength levels, thus a correspondingly large span of T_o. The ASTM Standard E 1921 [1] for measuring fracture toughness in the transition is based on the MC concept. However, there are a number of questions concerning the MC method. The most fundamental pertains to the existence of a universal MC shape, which is not understood [2]. Relevant background has been presented in previous reports, so a brief summary is given here.

Cleavage in steels involves a sequence of events ultimately associated with the unstable propagation of a microcracks formed at brittle trigger particle. The high stresses and strains in the blunting crack tip process zone crack these particles, such as grain boundary carbides. While many particles may exist in the process zone, only those with sufficiently large size and favorable orientation with respect to low toughness crystallographic planes and directions in the adjoining ferrite are 'eligible' for a microcrack propagation event. That is, the propagation versus arrest of a dynamic microcrack into the adjacent ferrite matrix is the critical event for macroscopic cleavage [3,4] and is associated with a critical stress, σ^*. The σ^* can be expressed in terms of a modified Griffith criteria in Equation 1 [2-4]:

$$\sigma^* = CK_{\mu}/\sqrt{d} \qquad (1)$$

Here, C is a geometric factor of order unity, that depends on the crack shape and d is the characteristic trigger particle size. Thus the macroscopic cleavage K_{Jc} is controlled, by the K_{μ} (<< K_{Jc}) of ferrite. The traditional model assumption is that σ^* is approximately independent of temperature. This assumption is consistent with MC behavior at low temperatures. However, at high temperatures and with $\Delta\sigma_y$ shifts caused by irradiation hardening this assumption is not consistent with observed MC shape. This inconsistency is a consequence of the decreasing temperature dependence of $\sigma_y(T)$ at higher $T_0 \geq \approx 0°C$, and can be remedied by incorporating a modest temperature dependence, as $\sigma^*(T)$.

The temperature dependence of $\sigma^*(T)$ demands a corresponding temperature dependence of $K_{\mu}(T)$. The fact that the position (T_o), but not the shape, of the MC depends on microstructure and alloy strength leads to the hypothesis that $K_{\mu}(T)$ is independent of the fine, nano-scale features introduced by irradiation. This further suggests that some intrinsic property of the ferrite matrix controls $K_{\mu}(T)$. Thus the focus of this work is on assessing $K_{\mu}(T)$ in Fe. While it can be inferred from the trigger particle size distribution and σ^*, K_{μ} cannot be directly measured [2-4]. However, it is possible to measure various toughness parameters of single crystal Fe oriented for cleavage, including the static (K_{Ic}) and dynamic (K_{Id}) initiation toughness for sharp cracks, and the arrest toughness (K_{Ia}) for propagating cracks. While not identical properties, we propose that the $K_a(T)$ is a good surrogate for $K_{\mu}(T)$.

In spite of the paucity of data, many models have been proposed to describe the BDT in Fe and other bcc metals and alloys. Regardless of detail and level of approximation, however, most BDT models are based on the interaction between a (usually) sharp crack tip under increasing remote loading (K_I) and the evolution of local dislocation structures. The first successful attempt to model the BDT, based on an energy criterion mediating the nucleation of a single dislocation (ductile) prior to bond breaking (brittle), was proposed by Rice and Thomson (RT) [5]. The RT model and its progeny focusing on the nucleation and glide of dislocations, coupled with some detailed experimental observations, have helped to clarify the specific crystallographic slip processes involved in shielding a stationary crack tip. However, the various BDT models involve a number of assumptions and approximations and predict a wide range of behavior. The models and model parameters can be adjusted to match wide range of experimental results. Further, the BDT models have generally not addressed the crack tip processes involved in continued propagation of a cleavage crack, or arrest of the crack by the evolution of crack tip shielding dislocations. Thus, it is clear that the atomic level processes that govern the BDT are not fully understood in general, and for crack arrest in particular. Hence, our major objective is to develop a unique toughness database of unalloyed Fe single crystals over a wide range of temperature.

Experimental Procedure

The following section only very briefly outlines the challenging experimental techniques used in this study, and greater detail is given in previous reports. Single crystal rods sectioned into thin rectangular slices with the desired (100)[010], (100)[011], (110)[001] and (110)[110] cleavage orientations were procured from Monocrystals Co. The slices were incorporated into composite specimens reflecting two different approaches to testing, referred to as the 'bridge' and 'wedge' techniques. In both cases, the composite specimens were fabricated by diffusion bonding the single crystal slices to high strength steel sections that served both to transmit loads and store and release elastic energy.

The bridge technique was a modified compression precracking method, where the beam initially contains a shallow fatigue pre-crack [6]. Figure 1 (blue line) shows the variation in the corresponding normalized stress intensity factor ($K_I/\sigma W^{1/2}$) versus the crack depth to beam width ratio (a/W) determined from a detailed finite element (FE) analysis. The major limitation of the compression anvil bridge technique is that at higher test temperatures (T > -100°C) it is not possible to initiate a dynamic crack from a shallow fatigue pre-crack at a compressive σ that does not damage or deform the specimen.

Thus a second method was developed based on the wedge loading of a composite chevron specimen with short double cantilever arms [7]. The wedge technique allowed access to higher test temperatures up to ≈ 0°C, and has the advantage that multiple initiation and arrest events can be measured with a single specimen. Implementation of this test method also required a detailed FE analysis and optimization, leading to the normalized stress intensity factor ($K_I B^{1/2}/E\Delta$) shown by Figure 1 (red lines), where Δ is the wedge opening displacement at the end of the beam arms. One very important detail about the double cantilever beam chevron wedge test determined in the FE analysis was that the K_I is higher at the edge corners (solid red line) of the crack front in the chevron than in the center (dashed red line). Thus cracks tend to initiate at the corners (at K_{Ic}) and arrest (at K_{Ia}) in the middle of the crack front.

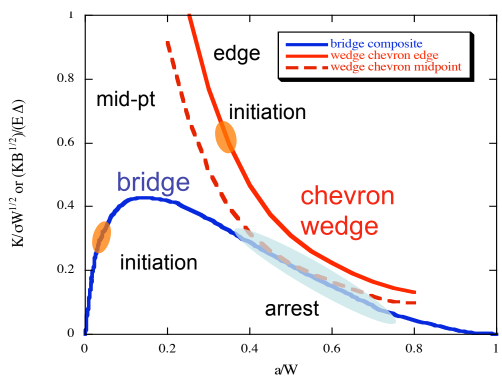

Figure 1. Finite element assessment of the stress intensity for the bridge and wedge specimens.

Following bridge testing, the beam specimens are left with a deep and very sharp pre-crack, providing the opportunity to obtain initiation toughness measurements over a range of loading rates from static (K_{Ic}) to dynamic (K_{Id}). The initiation tests were carried out in 4-point bending through servo-hydraulic load frame and drop tower loading schemes at $\dot{K}$ from ≈ 1-10^4 MPa√m/s. Note the corresponding $\dot{K}$ for the chevron wedge specimen tests was ≈ 0.1 MPa√m/s thereby increasing the overall $\dot{K}$ range of this study.

Results

The average K_{Ia} results for the four cleavage orientations are shown in Figure 2. The standard deviations of the K_{Ia} data scatter are not shown, but are in the range of ±1.0 to1.5 MPa√m. There is good agreement between the two techniques, so the data is combined where they overlap below -100°C. The (100)[011] orientation is in general slightly lower than the (100)[010], and the (100) plane data is much lower that the (110). Also the transition for the (100) plane data occurs at a higher temperature than the (110) plane. However, while an attempt was made to force cleavage onto the (110) planes, the cracks always propagated along the (100) plane. Therefore, the toughness levels are not truly representative of this cleavage system.

The results of the (100) plane K_{Id} over the range of $\dot{K}$ = 0.1-10^4 MPa√m/s are summarized in Figure 3a. In general the [011] direction is slightly less tough than the [010], but they are very similar and are combined to reflect the (100) plane. As expected, the K_{Id} decrease with rising $\dot{K}$.

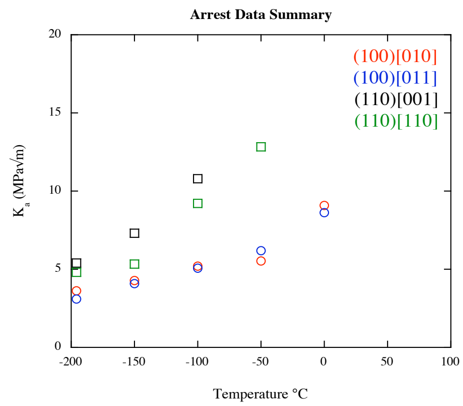

Figure 2. Results of arrest toughness measurements on Fe single crystal.

It is expected that the $\dot{K}$ dependence of K_{Id} derives from the corresponding strain rate dependence of σ_y (or, more precisely, the critical resolved shear stresses for the glide of screw dislocations on pertinent slip systems). To test this hypothesis the data from Figure 3a, along with the K_{Ic} from the double cantilevered beam chevron wedge specimen test are re-plotted in Figure 3b on a $\dot{K}$ compensated temperature scale T', analogous to a strain rate compensated temperature. T' (°K) is given by:

$$T' = T[1 - C\ln(\dot{K}/\dot{K}_r)]. \qquad (2)$$

Here $\dot{K}$ is the loading rate for a specific test and $\dot{K}_r$ is a reference rate of 1000 MPa√m/s. The C is 0.035 consistent with the corresponding strain rate dependence of σ_y. While the data remain scattered, the $K_{Ic/d}$ data fall in a common band, except possible at the lowest temperature where the K_{Ic} data remains higher than the K_{Id} results. However, These results lend powerful support to the hypothesis that the BDT in Fe (and other bcc metals and alloys) is controlled by thermally activated dislocation glide processes.

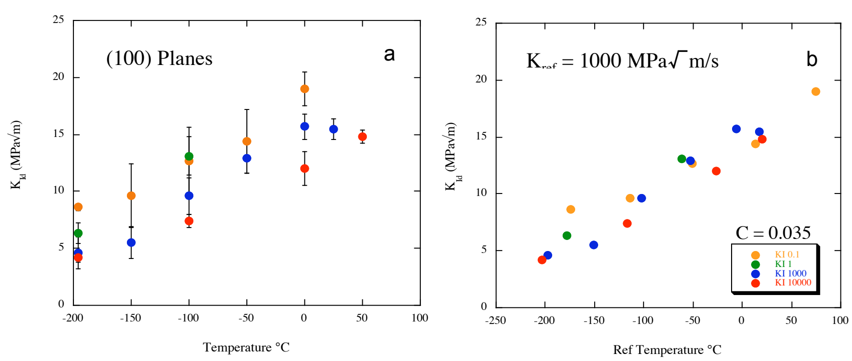

Figure 3a-b. a) Results of (100) planar orientation rate effect dynamic toughness study. b) Rate adjustment of dynamic data to a reference state similar to a strain rate compensated σ_y.

Figure 4 compares K_{Ic} data from each of the orientations in the quasi-static loading condition (0.1 MPa√m/s) to that of W single crystals reported by Gumbsh [8] plotted on a homologous T/T_m scale, where T_m is the melting temperature. Overall the initiation toughness data are similar, with the exception of the (110)[110] system, but issues with the (110) plane data have been addressed. At low temperatures, the W data are somewhat lower than the Fe K_{Ic} data. Agreement is better at higher temperatures although an abrupt BDT for W occurs at a lower T/T_m.

Figure 5a compares the K_{Ia} data for Fe and Fe-3wt%Si single crystal reported by Argon (unfilled diamonds) [9]. At comparable K_{Ia} levels the Fe data (green circles) is ≈ 150°C lower in temperature. This difference could be rationalized by the solid solution strengthening contribution of the 3%Si to the alloy σ_y (or, more properly, the critical resolved shear stresses for screw

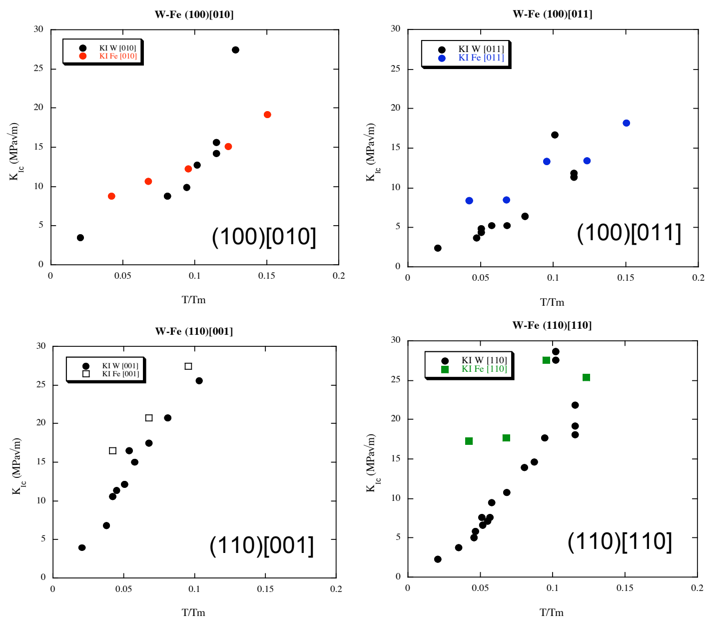

Figure 4. Comparison of quasi-static K_{Ic} Fe and W data on four low toughness orientations.

dislocation glide on the pertinent slip systems) compared to unalloyed Fe. If it is assumed that the Si contribution to the thermally activated (rate dependent) lattice resistance to dislocation slip is similar in consequences to the crystal lattice contribution (the Pieirls stress) in unalloyed Fe at lower temperatures, the corresponding temperature shift in the K_{Ia} can be evaluated at the difference in the temperatures, ΔT, for equivalent σ_y in Fe and Fe-3wt%Si [10]. The corresponding ΔT is estimated to be ≈ 150°C, as shown by the red symbols in Figure 5a, which are in good agreement with the Fe-3wt%Si K_{Ia} data. Note, Si is spaced less than one nm apart on the slip and two adjoining planes, hence, might be expected to produce a friction like lattice resistance stress. There are, however, complications in this simple hypothesis, like the fact that Si produces softening at low temperatures. Thus additional research is needed to understand the role of solutes in mediating the BDT.

Figure 5b compares the Fe $K_{Ia}(T)$ data to the $K_\mu(T)$ derived (blue line) from a fitted $\sigma^*(T)$ that is consistent with an invariant MC shape in low alloy C-Mn-Mo-Si-Ni and C-Cr-Mo-W steels. As in the case with the Fe-3wt%Si K_{Ia} data, the $K_\mu(T)$ data (green circles) are either: a) simply totally inconsistent with the measured $K_{Ia}(T)$ for Fe; or b) the $K_{Ia}(T)$ in typical alloys are shifted up (red circles) in temperature by approximately 220°C, due to mechanisms such as solid solution strengthening and, possibly, long range stress fields. Of course, the latter interpretation is not fully consistent with our previous hypothesis that there is a completely intrinsic $K_{Ia}(T)$-BDT curve for ferrite that is relatively independent of the microstructure, such as changes induced by irradiation. Further, even with a large shift the adjusted Fe K_{Ia} data show a somewhat stronger temperature dependence than the normalized $K_\mu(T)$ curve, especially at the highest temperature. However, it is noted that the $K_\mu(T)$ curve depends on the assumed temperature dependence of σ_y, which was taken from the average of many steels and other details that are not accounted for in this simple analysis, like the effects of temperature and irradiation on strain hardening as well as the effective strain rate in the process zone. Further, there is little valid K_{Jc} data to test the hypothesis of a MC shape at temperatures above ≈ 100°C.

A weak effect of microstructure versus a stronger effect of solutes on the BDT might be attributed to the corresponding difference between discrete, moderately strong to strong athermal dislocation obstacles that are much more widely spaced (typically > to >> ≈ 10 nm) compared to closely spaced (< 1 nm) dissolved solutes, that contribute to a thermally activated and rate dependent lattice friction type flow stress. Finally, we re-emphasize that $K_a(T)$ and $K_\mu(T)$ are not identical properties, and possible differences between them will also be explored in the future. Thus the solute BDT temperature shift concept is a plausible but not proven hypothesis.

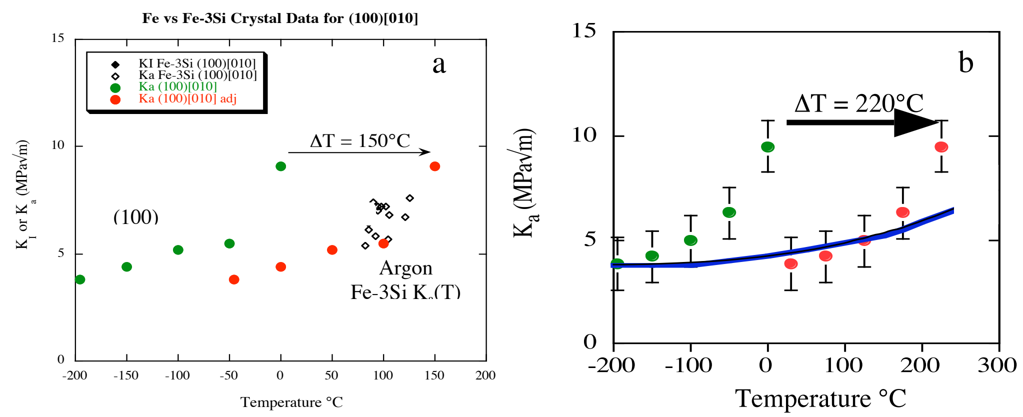

Figure 5a-b. a) Comparison of Fe and Fe-3Si arrest toughness levels showing an approximate 150°C difference in equivalent toughness levels. b) Comparison of Fe arrest toughness to that predicted to alleviate discrepancy between model and observed MC shape.

Future Work

The toughness measurements will be complemented by detailed characterization of the fracture surface features, side slip traces, and dislocation structures using optical and scanning electron microscopy. The main goal is develop a catalog of images from combinations of orientation, temperature and applied loading rate. The results of the characterization studies will be correlated with general trends in fracture surface topology, such as arrest front depth, apparent amount of dislocation activity on the surface, and size of the arrest/re-initiation boundary. Finally, etch pit studies of fracture and side slip surfaces have been initiated in attempt to identify the type of dislocations active and quantify the dislocation densities of the various regions of the crack trace.

References

[1] ASTM Standard E 1921-97, ASTM 2003.
[2] G. R. Odette and M. Y. He, J. Nucl. Mater. 283-287 (2000) 120.
[3] G. R. Odette, T. Yamamoto, H. J. Rathbun, M. L. Hribernik, and J. W. Rensman, J. Nucl. Mater. 323 (2003) 313.
[4] G. T. Hahn, Metall. Trans. 15A (1984) 987.
[5] J. R. Rice and R. Thomson, Philos. Mag. 29 (1974) 73.
[6] ASTM Standard C 1421-99, ASTM 2000.
[7] ASTM Standard E 1304-97, ASTM 1998.
[8] P. Gumbsch, J. Riedle, A. Hartmaier, and H. F. Fischmeister, Science 282 (1998) 1293.
[9] Y. Qiao and A. S. Argon, Mech. Mater. 35 (2003) 903.
[10] P. B. Pickering, in Physical Metallurgy and the Design of Steels (1978) 65.